

25
p

CAT. 29

N64-20818

code 1

NASA CW56169

Technical Report No. 32-577

*Unified Guidance Analysis in Design
of Space Trajectories*

T. T. Soong

C. G. Pfeiffer

R. Hamburg

OTS PRICE

XEROX

\$ 260 ph

jpl

JET PROPULSION LABORATORY
CALIFORNIA INSTITUTE OF TECHNOLOGY
PASADENA, CALIFORNIA

January 31, 1964

Technical Report No. 32-577

*Unified Guidance Analysis in Design
of Space Trajectories*

T. T. Soong

C. G. Pfeiffer

R. Hamburg

T. W. Hamilton

*T. W. Hamilton, Chief
Systems Analysis*

JET PROPULSION LABORATORY
CALIFORNIA INSTITUTE OF TECHNOLOGY
PASADENA, CALIFORNIA

January 31, 1964

Copyright © 1964
Jet Propulsion Laboratory
California Institute of Technology

Prepared Under Contract No. NAS 7-100
National Aeronautics & Space Administration

CONTENTS

I. Introduction	1
II. Scope of Guidance Analysis and Basic Equations	2
III. General Properties of Differential Corrections	3
A. A Factorization of the K Matrix: Dimensionless Differential Corrections	3
B. Diagonalization of the K Matrix: The "Proper" Coordinate System	4
C. Dispersion Ellipsoids	5
D. Capability of Midcourse Correction	5
IV. Numerical Results	6
Nomenclature	16
Appendix	17
References	19

FIGURES

1. The coordinate system	6
2. Max gradient vs time angle for eccentricity 0.0	7
3. Min gradient vs time angle for eccentricity 0.0	7
4. Normal gradient vs time angle for eccentricity 0.0	7
5. Gradient angle vs time angle for eccentricity 0.0	7
6. Target angle vs time angle for eccentricity 0.0	8
7. Max gradient vs time angle for eccentricity 0.1	8
8. Min gradient vs time angle for eccentricity 0.1	8
9. Normal gradient vs time angle for eccentricity 0.1	8
10. Gradient angle vs time angle for eccentricity 0.1	9
11. Target angle vs time angle for eccentricity 0.1	9
12. Max gradient vs time angle for eccentricity 0.25	9
13. Min gradient vs time angle for eccentricity 0.25	9
14. Normal gradient vs time angle for eccentricity 0.25	10
15. Gradient angle vs time angle for eccentricity 0.25	10

FIGURES (Cont'd)

16. Target angle vs time angle for eccentricity 0.25	10
17. Max gradient vs time angle for eccentricity 0.5	10
18. Min gradient vs time angle for eccentricity 0.5	11
19. Normal gradient vs time angle for eccentricity 0.5	11
20. Gradient angle vs time angle for eccentricity 0.5	11
21. Target angle vs time angle for eccentricity 0.5	11
22. Max gradient vs time angle for eccentricity 0.75	12
23. Min gradient vs time angle for eccentricity 0.75	12
24. Normal gradient vs time angle for eccentricity 0.75	12
25. Gradient angle vs time angle for eccentricity 0.75	12
26. Target angle vs time angle for eccentricity 0.75	13
27. Max gradient vs time angle for eccentricity 0.9	13
28. Min gradient vs time angle for eccentricity 0.9	13
29. Normal gradient vs time angle for eccentricity 0.9	13
30. Gradient angle vs time angle for eccentricity 0.9	14
31. Target angle vs time angle for eccentricity 0.9	14
32. Max gradient vs time angle for eccentricity 0.98741	14
33. Min gradient vs time angle for eccentricity 0.98741	14
34. Normal gradient vs time angle for eccentricity 0.98741	15
35. Gradient angle vs time angle for eccentricity 0.98741	15
36. Target angle vs time angle for eccentricity 0.98741	15

ABSTRACT

20818

A

Based on the fact that all ballistic space trajectories can be piecewise approximated by conic sections, certain geometric and dynamic similarities of these trajectories permit a systematic and unified guidance investigation. This Report develops a set of dimensionless differential corrections and a "proper" coordinate system suitable for generalized guidance analysis. Numerical results in graphic form are presented which are applicable to the calculation of target dispersions due to random injection errors and the determination of required mid-course corrective maneuvers.

*Author***I. INTRODUCTION**

In planning a lunar or planetary mission, numerous preflight trajectories are generated to find a set of standard trajectories that best accommodates mission objectives and that also meets guidance and tracking requirements. It is clear that as the complexity and intensity of space exploration increases, a unified approach to trajectory design must be developed to minimize the task of the trajectory designers. A major step in this unifying attempt has been the use of Keplerian conic sections to approximate various segments of a space trajectory (Ref. 1, 2). This approach to trajectory calculation greatly reduces the computing time and gives accurate trajectory representation for many design purposes. Using conic approximations, a space trajectory can be logically divided into

distinct phases. An interplanetary trajectory, for example, consists of three phases of Keplerian motion: an escape hyperbola near the launch planet, a transfer ellipse under the influence of the Sun, and an approach hyperbola near the target planet. A lunar trajectory consists of a transfer ellipse from the Earth to the vicinity of the Moon, and an approach hyperbola near the Moon. In both cases, the transfer ellipse is the major portion of the trajectory, and determines its essential characteristics.

This Report is concerned with the unified treatment of trajectory design from the guidance point of view, the objective being to study the target error sensitivity to velocity impulses at various points along the path. The

approach presented is based on the usual assumption that the actual trajectory followed by a spacecraft differs only slightly from the designed or standard trajectory so that linear perturbation theory is adequate for error analysis. Within the framework of linear theory, the guidance characteristics are then determined by the behavior of the set of differential corrections which map velocity perturbations to target errors. It is further assumed that, while the escape and approach hyperbolic conics are important in design studies of launch and arrival phases of flight, they may be ignored for guidance investigation, and only the transfer ellipse need be con-

sidered. This assumption greatly facilitates the generalization of guidance analysis, and guidance studies for lunar and planetary missions (Ref. 3) have shown that such an approximation is adequate for many design purposes.

Following this approach, this Report develops a set of dimensionless differential corrections, permitting a systematic and unified guidance investigation of the transfer ellipse. In order to facilitate the exposition, a "proper" coordinate system suitable for guidance studies is introduced. Numerical results in graphic form are presented.

II. SCOPE OF GUIDANCE ANALYSIS AND BASIC EQUATIONS

Because of error sources in the injection guidance system, a space vehicle designed to reach a desired terminal point at a given time on the standard (or reference) trajectory will generally not achieve the desired terminal conditions unless corrective maneuvers are made. Space guidance is accomplished by employing an orbit determination process to estimate the orbital elements of the trajectory, and then applying one or more impulsive velocity corrections to null the predicted target error. Given a designed trajectory, the preflight guidance analysis deals primarily with the statistical problems of (1) examining the target dispersions arising from errors in the injection guidance system, the orbit determination process, and the commanded corrections, and (2) determining the amount of propellant to carry aboard the spacecraft for corrective maneuvers. Since the basic guidance theory has been well documented (Ref. 4, 5), the present work will only state some basic equations pertaining to the analysis to follow.

In the absence of postinjection guidance, the position error vector $\delta \mathbf{r}_t$ at targeting time t_t is a function of the standard trajectory and the errors at injection. Assuming linear perturbation theory to be valid, $\delta \mathbf{r}_t$ is given by

$$\delta \mathbf{r}_t = U_0 \delta \mathbf{q}_0 = \left[\frac{\partial \mathbf{r}_t}{\partial \mathbf{q}_0} \right] \delta \mathbf{q}_0 \quad (1)$$

where $\delta \mathbf{q}_0$ is the six-dimensional (position and velocity) error vector at injection time t_0 , and U_0 is a 3 by 6 mapping matrix evaluated on the standard trajectory. In order to correct the target miss by applying a velocity impulse $\Delta \mathbf{v}_t$ at some time t after injection we have

$$\Delta \mathbf{v}_t = -K_t^{-1} \delta \mathbf{r}_t = -K_t^{-1} U_0 \delta \mathbf{q}_0 \quad (2)$$

where

$$K_t = \left[\frac{\partial \mathbf{r}_t}{\partial \mathbf{v}_t} \right]$$

is a 3 by 3 mapping matrix. The inflight calculation of "velocity-to-be-gained" $\Delta \mathbf{v}_t$ is given by Eq. (2), where $\delta \mathbf{q}_0$ is estimated from the orbit determination process.

Since $\delta \mathbf{q}_0$ can only be described statistically in preflight studies, the amount of propellant required for corrective maneuvers is determined from Eq. (2) by considering the covariance matrix of $\Delta \mathbf{v}_t$, given the covariance matrix of $\delta \mathbf{q}_0$. Let

$$\Lambda_{vt} = \langle \Delta \mathbf{v}_t \Delta \mathbf{v}_t^T \rangle$$

and

$$\Lambda_0 = \langle \delta \mathbf{q}_0 \delta \mathbf{q}_0^T \rangle$$

where the superscript T indicates "transpose" and the angle brackets indicate ensemble average. It follows from Eq. (2) that

$$\Lambda_{vt} = K_t^{-1} U_0 \Lambda_0 U_0^T (K_t^{-1})^T \quad (3)$$

The trace of the matrix Λ_{vt} determines the mean-squared value of the required Δv_t at time t .

A commonly made assumption is that the position and velocity errors at injection can be represented by an "equivalent" velocity-to-be-gained Δv_0 . For example, Δv_0 would be the equivalent error in the hyperbolic excess velocity relative to the Earth for interplanetary missions. Equation (2) then reduces to

$$\Delta v_t = -K_t^{-1} K_0 \Delta v_0 \quad (4)$$

and Eq. (3) becomes

$$\Lambda_{vt} = K_t^{-1} K_0 \Lambda_0 K_0^T (K_t^{-1})^T \quad (5)$$

For subsequent guidance corrections the errors in applying the first correction, due to orbit determination and maneuver mechanization, play the role of Δv_0 .

It can be seen that, given the statistics of the injection errors for any standard trajectory, preflight guidance analysis of the mission is based upon the properties of K_t for $t_0 \leq t \leq t_{\text{final}}$. Hence, the unified approach to preflight guidance analysis hinges on the general properties of K_t over the set of all possible transfer ellipses. It is recalled that the elements of K_t are simply the partial derivatives of position coordinates at a terminal time t_f with respect to the velocity coordinates at some previous time t . This set of partial derivatives shall be called differential corrections. Their general properties and numerical results pertaining to a unified guidance investigation are discussed in the Sections to follow.

III. GENERAL PROPERTIES OF DIFFERENTIAL CORRECTIONS

In this Section let us consider in general the 3 by 3 matrix $K(t_2, t_1)$, defined by

$$\delta r(t_2) = K(t_2, t_1) \delta v(t_1) \quad t_2 \geq t_1 \quad (6)$$

where $\delta v(t_1)$ is a small perturbation of the velocity vector at time t_1 on a designed trajectory, and $\delta r(t_2)$ is the corresponding position perturbation at some later time t_2 . For simplicity we write Eq. (6) in the form

$$\delta r_2 = K \delta v_1 \quad (7)$$

The assumption that the transfer ellipse gives adequate trajectory representation for guidance analysis purposes greatly facilitates the analytical determination of the differential corrections and, more important, makes possible the development of a set of generalized differential corrections applicable to a large class of space trajectories.

It also leads to the analytical determination of a coordinate system ideally suited for guidance studies.

A relatively simple derivation of the elements of K for an elliptic trajectory is given in the Appendix. This Report is primarily concerned with the general properties of the differential corrections so derived.

A. A Factorization of the K Matrix: Dimensionless Differential Corrections

If the trajectory from time t_1 to time t_2 is elliptic, the elements of K are uniquely determined when the following five parameters are specified:

μ = product of the gravitational constant and the mass of the central body

e = eccentricity

a = semimajor axis of the ellipse

ϕ_1 and ϕ_2 = angle coordinates (true anomalies, eccentric anomalies, or mean anomalies) of the space vehicle at times t_1 and t_2 respectively.

Hence we may write

$$\delta \mathbf{r}_2 = K(\mu, a, e, \phi_2, \phi_1) \delta \mathbf{v}_1 \quad (8)$$

Since dimensional homogeneity of Eq. (8) requires that the elements of K have the dimension of time, it is immediately revealed from dimensional analysis that a factorization exists, namely,

$$K(\mu, a, e, \phi_2, \phi_1) = \frac{1}{n} K'(e, \phi_2, \phi_1) \quad (9)$$

where $n = [\mu/a^3]^{1/2}$ is the mean angular velocity. The elements of K' are dimensionless. This observation is important as it implies that for two elliptic orbits with the same eccentricity we have the relation

$$K_1(\phi_2, \phi_1) = \frac{n_1}{n_2} K_2(\phi_2, \phi_1) \quad (10)$$

The dimensionless elements of K' are of central importance, since the differential corrections for a whole class of trajectories having the same eccentricity can be obtained from them by the multiplication of a simple factor $1/n$.

B. Diagonalization of the K Matrix: The "Proper" Coordinate System

In the study of differential corrections and guidance characteristics, great mathematical simplicity results when, by means of proper choices of orthogonal coordinate systems for $\delta \mathbf{v}_1$ and $\delta \mathbf{r}_2$, the K matrix becomes diagonal. To illustrate, let

$$\delta \mathbf{v}_1^T = (\delta v_1, \delta v_2, \delta v_3) \quad (11)$$

and

$$\delta \mathbf{r}_2^T = (\delta r_1, \delta r_2, \delta r_3)$$

where the coordinate systems describing \mathbf{v}_1 and \mathbf{r}_2 are chosen so that

$$K = \text{diag}(\lambda_1, \lambda_2, \lambda_3) \quad (12)$$

The matrix Eq. (7) then reduces to

$$\delta r_j = \lambda_j \delta v_j \quad j = 1, 2, 3 \quad (13)$$

The linear mapping properties between the two vector variations $\delta \mathbf{v}_1$ and $\delta \mathbf{r}_2$, either in the statistical or deterministic sense, now become immediately apparent. We shall now show that there exist orthogonal coordinate systems for $\delta \mathbf{v}_1$ and $\delta \mathbf{r}_2$ where a diagonal K matrix results, and present formulas for their analytical determination.

Let us consider the Cartesian coordinate system shown in Fig. 1, i.e.,

$$\delta \mathbf{v}_1^T = (\delta \dot{x}_1, \delta \dot{y}_1, \delta \dot{z}_1) \quad (14)$$

$$\delta \mathbf{r}_2^T = (\delta x_2, \delta y_2, \delta z_2)$$

where x - and y -components are in the standard plane of motion and z -component is out-of-plane; then it is shown in the Appendix that

$$\frac{\partial x_2}{\partial \dot{z}_1} = \frac{\partial y_2}{\partial \dot{z}_1} = \frac{\partial z_2}{\partial \dot{x}_1} = \frac{\partial z_2}{\partial \dot{y}_1} = 0 \quad (15)$$

so that

$$\begin{bmatrix} \delta x_2 \\ \delta y_2 \\ \delta z_2 \end{bmatrix} = K \begin{bmatrix} \delta \dot{x}_1 \\ \delta \dot{y}_1 \\ \delta \dot{z}_1 \end{bmatrix} = \begin{bmatrix} k_{11} & k_{12} & 0 \\ k_{21} & k_{22} & 0 \\ 0 & 0 & k_{33} \end{bmatrix} \begin{bmatrix} \delta \dot{x}_1 \\ \delta \dot{y}_1 \\ \delta \dot{z}_1 \end{bmatrix} \quad (16)$$

It is thus obvious that the z -axis (out-of-plane direction) is one of the desired coordinate axes for both $\delta \mathbf{v}_1$ and $\delta \mathbf{r}_2$. Let us consider only in-plane coordinates, and define

$$\hat{K} = \begin{bmatrix} k_{11} & k_{12} \\ k_{21} & k_{22} \end{bmatrix} \quad (17)$$

Since a general real symmetric matrix can be reduced to diagonal form by means of an orthogonal transformation, we can find an orthogonal matrix

$$N_2 = \begin{bmatrix} \cos \alpha_2 & \sin \alpha_2 \\ -\sin \alpha_2 & \cos \alpha_2 \end{bmatrix} \quad (18)$$

such that

$$N_2 \hat{K} \hat{K}^T N_2^T = N_2 \begin{bmatrix} c & h \\ h & b \end{bmatrix} N_2^T = \begin{bmatrix} \lambda_1^2 & 0 \\ 0 & \lambda_2^2 \end{bmatrix} \quad (19)$$

It is easy to show that

$$\alpha_2 = \frac{1}{2} \tan^{-1} \frac{2h}{c-b} \quad (20)$$

The quadrant of α_2 is fixed if, for $\lambda_1 \neq \lambda_2$, we specify $\lambda_1 > \lambda_2$ and take the smallest $|\alpha_2|$ counterclockwise from some reference direction.

From Eq. (19) define the orthogonal transformation

$$N_1 = \begin{bmatrix} \frac{1}{\lambda_1} & 0 \\ 0 & \frac{1}{\lambda_2} \end{bmatrix} [N_2 \hat{K}] = \begin{bmatrix} \cos \alpha_1 & \sin \alpha_1 \\ -\sin \alpha_1 & \cos \alpha_1 \end{bmatrix} \quad (21)$$

which uniquely specifies α_1 if α_2 is given. Thus

$$N_1 N_1^T = \text{the identity} \quad (22)$$

and from Eq. (16),

$$\begin{aligned} N_2 \begin{bmatrix} \delta x_2 \\ \delta x_1 \end{bmatrix} &= N_2 \hat{K} (N_1^T N_1) \begin{bmatrix} \delta \dot{x}_1 \\ \delta \dot{y}_1 \end{bmatrix} \\ &= [N_2 \hat{K} \hat{K}^T N_2^T] \begin{bmatrix} \frac{1}{\lambda_1} & 0 \\ 0 & \frac{1}{\lambda_2} \end{bmatrix} [N_1] \begin{bmatrix} \delta \dot{x}_1 \\ \delta \dot{y}_1 \end{bmatrix} \\ &= \begin{bmatrix} \lambda_1 & 0 \\ 0 & \lambda_2 \end{bmatrix} [N_1] \begin{bmatrix} \delta \dot{x}_1 \\ \delta \dot{y}_1 \end{bmatrix} \end{aligned} \quad (23)$$

Hence, the K matrix becomes diagonal by choosing the initial and final coordinate system such that

$$\delta \mathbf{r}_2 = \begin{bmatrix} N_2 & 0 \\ 0 & 1 \end{bmatrix} \delta \mathbf{x}_2 \quad (24)$$

$$\delta \mathbf{v}_1 = \begin{bmatrix} N_1 & 0 \\ 0 & 1 \end{bmatrix} \delta \dot{\mathbf{x}}_1 \quad (25)$$

It is noteworthy that, since $1/n$ is a multiplicative factor of the K matrix, the angles α_1 and α_2 are functions only of e , ϕ_1 , and ϕ_2 .

C. Dispersion Ellipsoids

An important aspect to be considered is the determination of the probability density of position perturbations at time t_2 due to velocity variations at some previous time t_1 . Assuming that the $\delta \mathbf{v}_1$ has a multivariate Gaussian distribution with zero means and small standard deviations, it follows that the joint probability density of $\delta \mathbf{r}_2$ is also multivariate Gaussian. The position dispersions are conveniently expressed by three-dimensional dispersion ellipsoids determined by contours of constant probability density (Ref. 5). From Eq. (13) we conclude that the lengths of principal semiaxes of these ellipsoids are proportional to the λ_i and their orientations are given by the α_i if the components of $\delta \mathbf{v}_1$ are independent with equal standard deviations σ . Since the coordinates in the standard plane of motion are not coupled to out-of-plane coordinates, it is clear that one of the principal axes for all ellipsoids is the out-of-plane direction.

Let the lengths of the principal semiaxes of the cross section be denoted by λ_1^* and λ_2^* and that in the out-of-plane direction by λ_3^* ; then

$$\lambda_j^* = k \sigma \lambda_j \quad j = 1, 2, 3 \quad (26)$$

where k is the index of constant probability. For example, $k = 1, 2, 3$ would correspond to the probabilities 0.20, 0.74, and 0.94, respectively, of $\delta \mathbf{r}_2$ being within an ellipsoid.

D. Capability of Midcourse Correction

Given a position error $\delta \mathbf{r}_2$, which is to be corrected by a velocity impulse $\Delta \mathbf{v}_1$ at some time $t_1 < t_2$, the required $\Delta \mathbf{v}_1$ is [see Eq. (2)]

$$\Delta \mathbf{v}_1 = -K^{-1} \delta \mathbf{r}_2$$

if the K matrix is not singular. It is therefore of interest to examine the existence of K^{-1} for general elliptic trajectories.

The K matrix does not have an inverse if:

1. $\lambda_3 = 0$

The curves presented in Section IV indicate that this occurs when $\nu_2 - \nu_1$ is a multiple of π . It implies that an out-of-plane position error cannot be corrected by velocity impulses applied at $\nu_1 = \nu_2 - \pi$.

2. λ_2 and/or $\lambda_1 = 0$

This condition implies that the gradient vectors

$$\mathbf{g}_1 = \begin{bmatrix} k_{11} \\ k_{12} \end{bmatrix} \text{ and } \mathbf{g}_2 = \begin{bmatrix} k_{21} \\ k_{22} \end{bmatrix}$$

are collinear, or that one or both are zero.

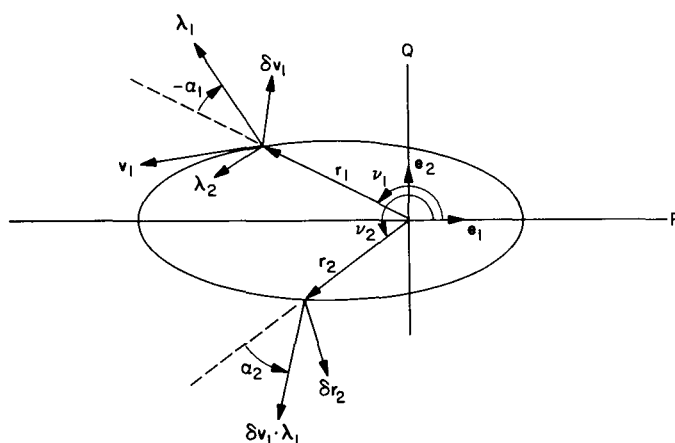


Fig. 1. The coordinate system

IV. NUMERICAL RESULTS

The elements of the diagonalized and normalized differential correction matrix λ'_i and the coordinate rotation angles α_i were numerically evaluated with an IBM 7094 digital computer, based on the analytical expressions derived in the Appendix. These quantities were then plotted automatically, and are presented in graphic form in Fig. 2-36. Their definitions are as follows:

Max gradient = maximum of $\{\lambda'_1, \lambda'_2\}$, where $\lambda'_i = n\lambda_i$ and λ_1, λ_2 are defined by Eq. (19)

Min gradient = minimum of $\{\lambda'_1, \lambda'_2\}$

Normal gradient = the out-of-plane differential correction $\lambda'_3 = nk_{33}$, where k_{33} is defined by Eq. (16)

Gradient angle = the rotation angle α_1 [Eq. (21)], measured counterclockwise from \mathbf{r}_1 to the maximum gradient vector (Fig. 1)

Target angle = the rotation angle α_2 [Eq. (18)], measured counterclockwise from \mathbf{r}_2 to target error direction $\delta \mathbf{v}_1 \cdot \boldsymbol{\lambda}_1$ (Fig. 1)

Since the dimensionless differential corrections are functions of the eccentricity of the ellipse and the angle

coordinates of the space vehicle at the initial and final points of the trajectory, a large collection of graphs is necessary to cover various practical situations (Fig. 2-36). The graphs are constructed by choosing seven values of the eccentricity: $e = 0, 0.1, 0.25, 0.5, 0.75, 0.9$ and 0.98741 (a typical value for lunar trajectories). For each value of e several final target positions are chosen, defined by the true anomaly ν_2 at multiples of 30-deg intervals from 0 to 360 deg. The above-described quantities are then presented for various values of ν_2 by plotting them vs the difference between the final and initial mean anomalies (in degrees), which is called "time angle." The time angle divided by the mean angular velocity (in compatible units) is the time of flight between the initial and final point. For the circular orbit case ($e = 0$) only one curve is presented for each quantity considered, since the differential corrections are not functions of ν_2 explicitly. Note that the choice of time as independent variable (rather than, say, true anomaly) implies that the differential corrections do not all go to zero at a time angle equal to 360 deg.

A thorough interpretation of the numerical results is beyond the scope of this Report, but some discussion is in order to explain the unusual behavior of the curves for

eccentricity near one (see Fig. 32-36). On rectilinear ellipses ($e = 1$) the velocity vector instantaneously rotates by 180 deg at apopsis and periapsis, and at periapsis the speed becomes infinite. Recognizing that the differential corrections are the partial derivatives of position coordinates at some fixed time with respect to velocity coordinates at some earlier fixed time, and that the semimajor axis of the ellipse can be changed only by

applying a velocity perturbation in the direction of the velocity vector, the behavior of the curves for eccentricity near one can be intuitively justified.

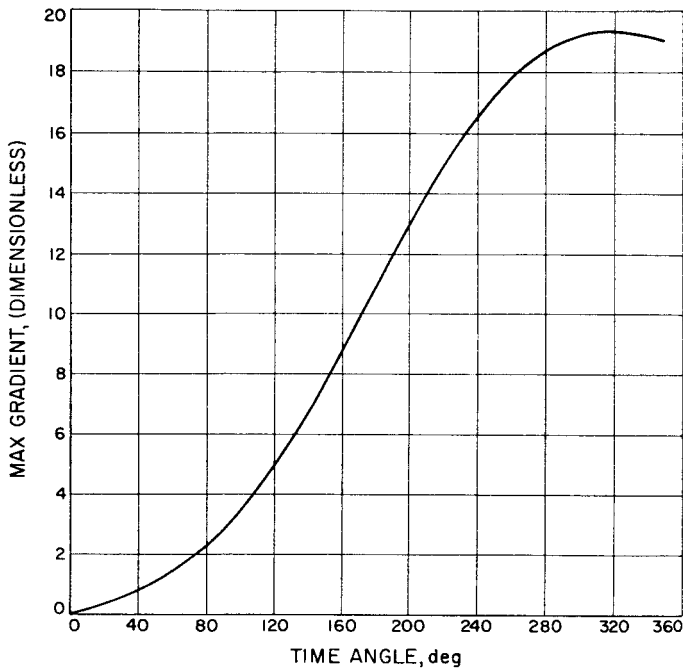


Fig. 2. Max gradient vs time angle for eccentricity 0.0

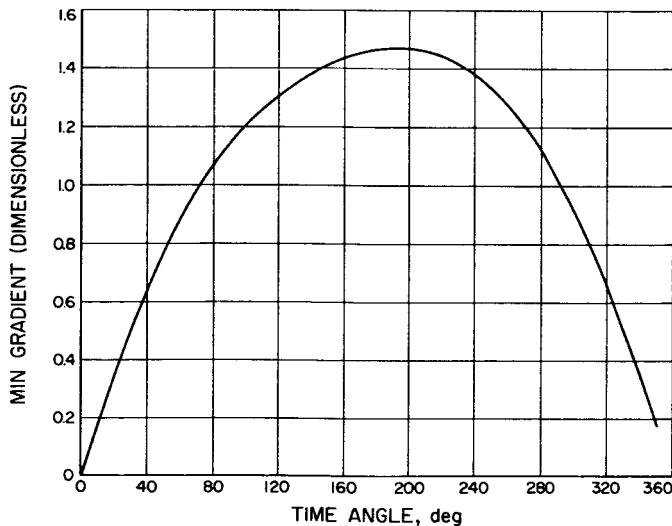


Fig. 3. Min gradient vs time angle for eccentricity 0.0

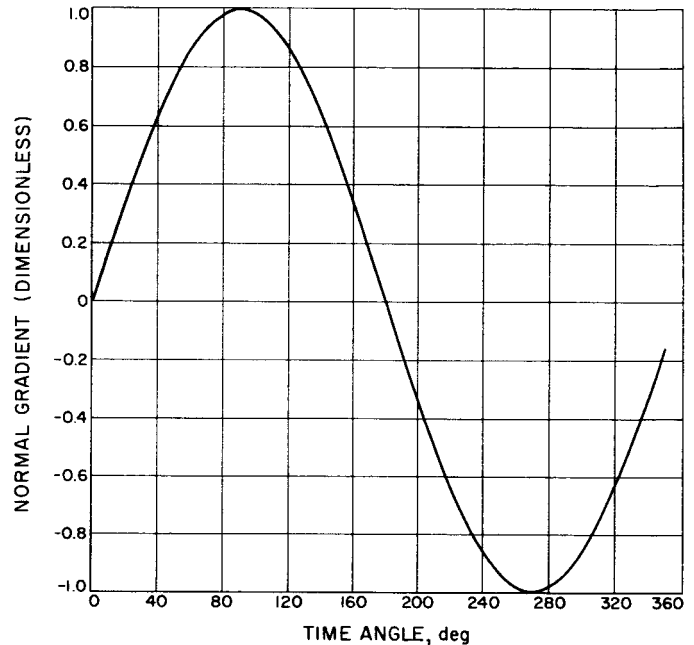


Fig. 4. Normal gradient vs time angle for eccentricity 0.0

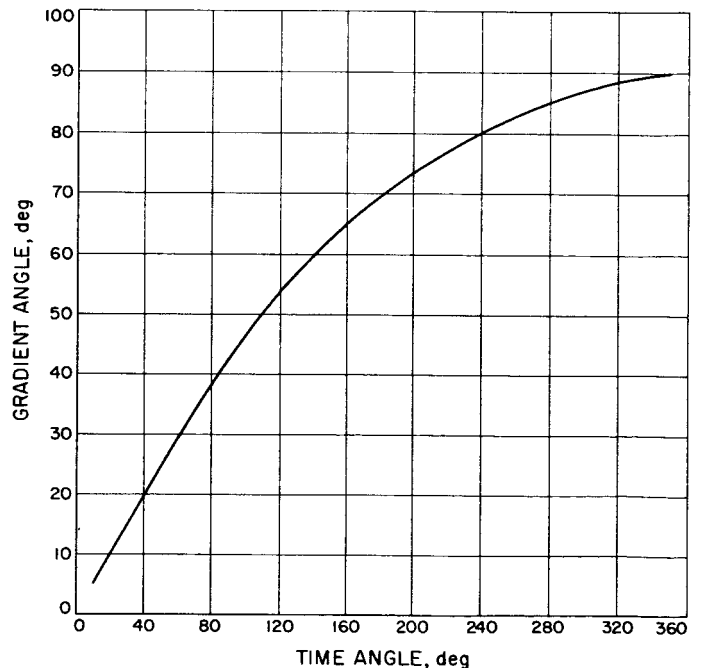


Fig. 5. Gradient angle vs time angle for eccentricity 0.0

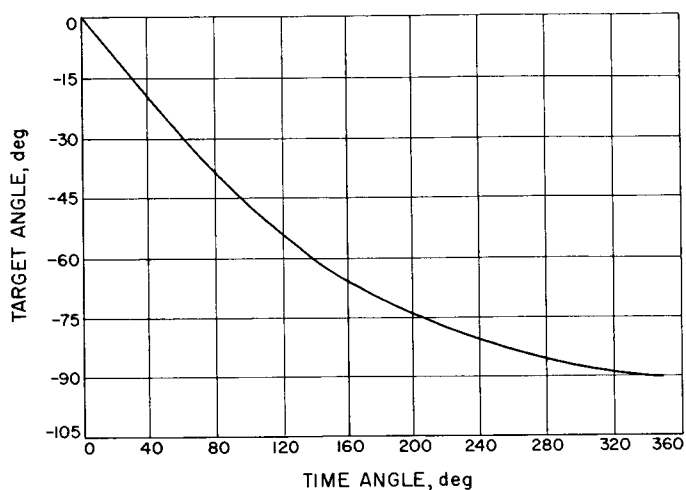


Fig. 6. Target angle vs time angle for eccentricity 0.0

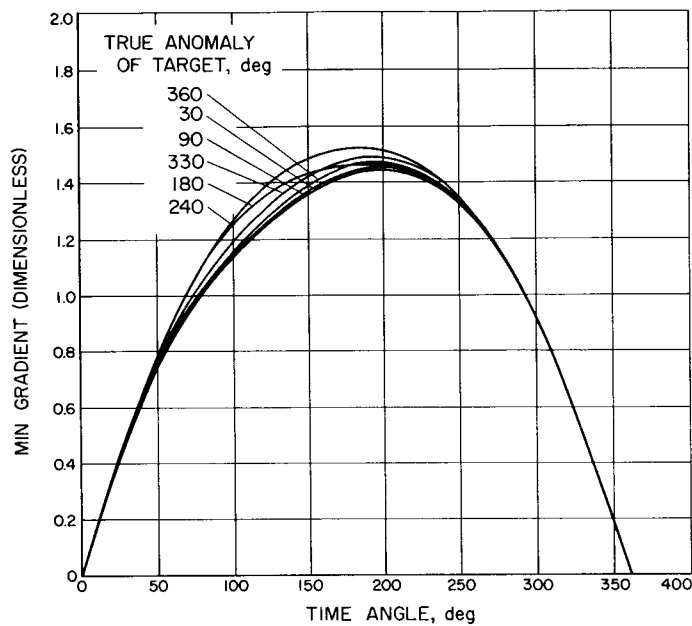


Fig. 8. Min gradient vs time angle for eccentricity 0.1

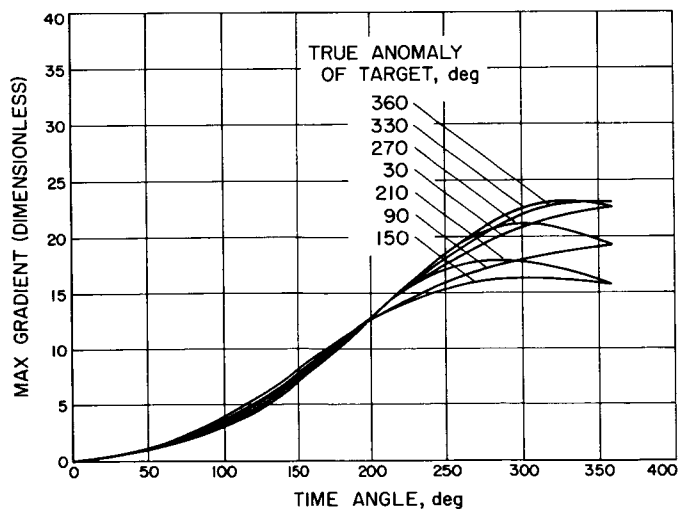


Fig. 7. Max gradient vs time angle for eccentricity 0.1

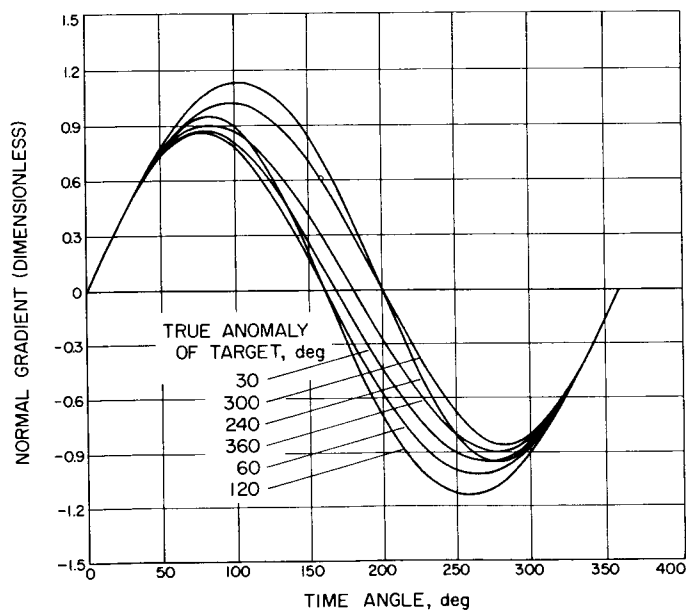


Fig. 9. Normal gradient vs time angle for eccentricity 0.1

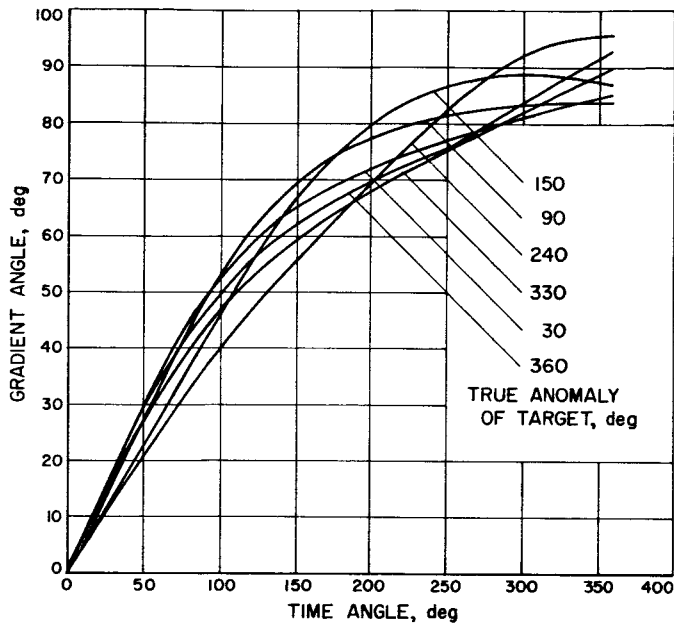


Fig. 10. Gradient angle vs time angle for eccentricity 0.1

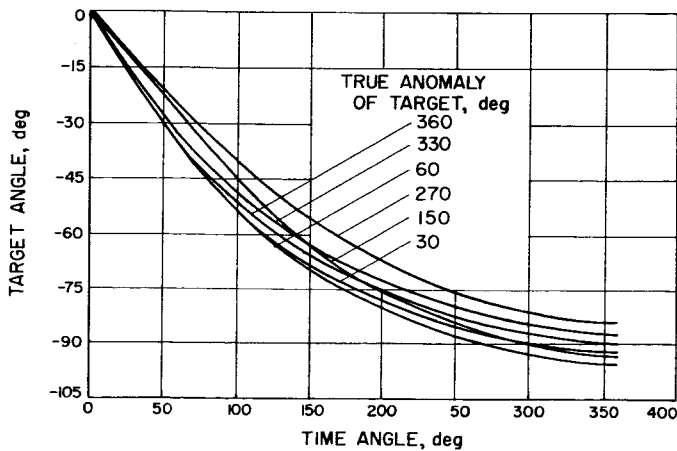


Fig. 11. Target angle vs time angle for eccentricity 0.1

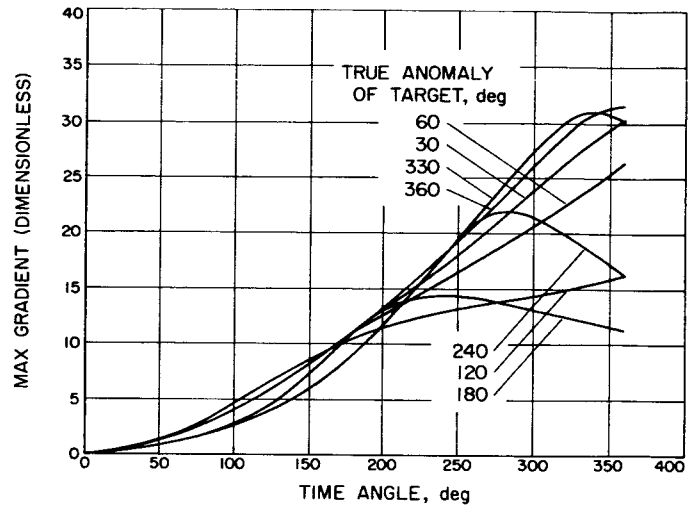


Fig. 12. Max gradient vs time angle for eccentricity 0.25

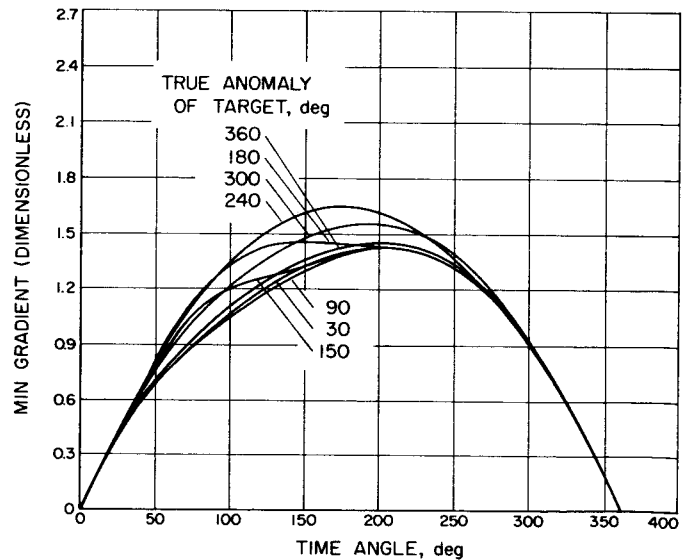


Fig. 13. Min gradient vs time angle for eccentricity 0.25

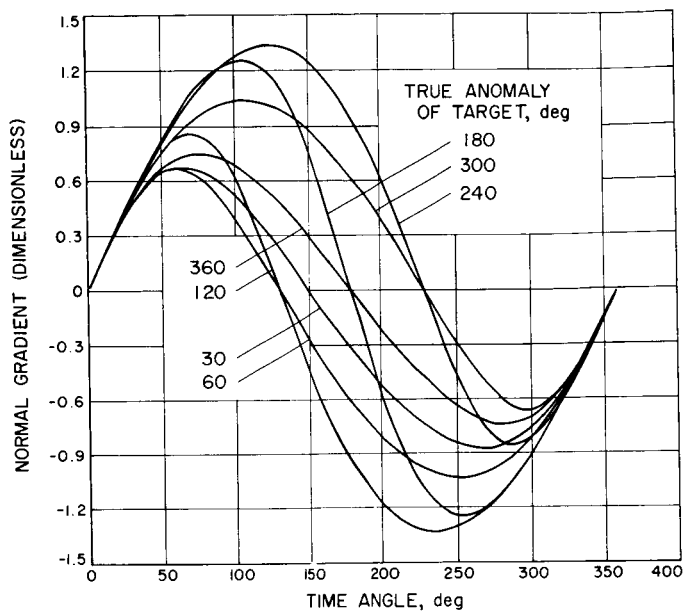


Fig. 14. Normal gradient vs time angle for eccentricity 0.25

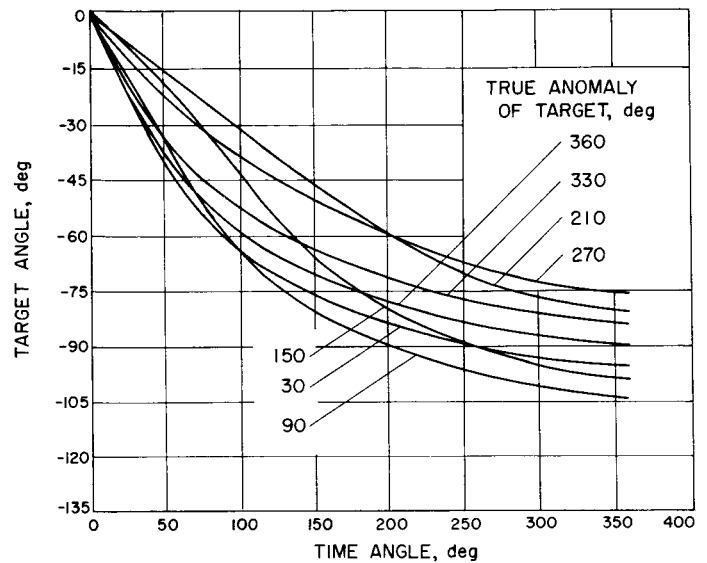


Fig. 16. Target angle vs time angle for eccentricity 0.25

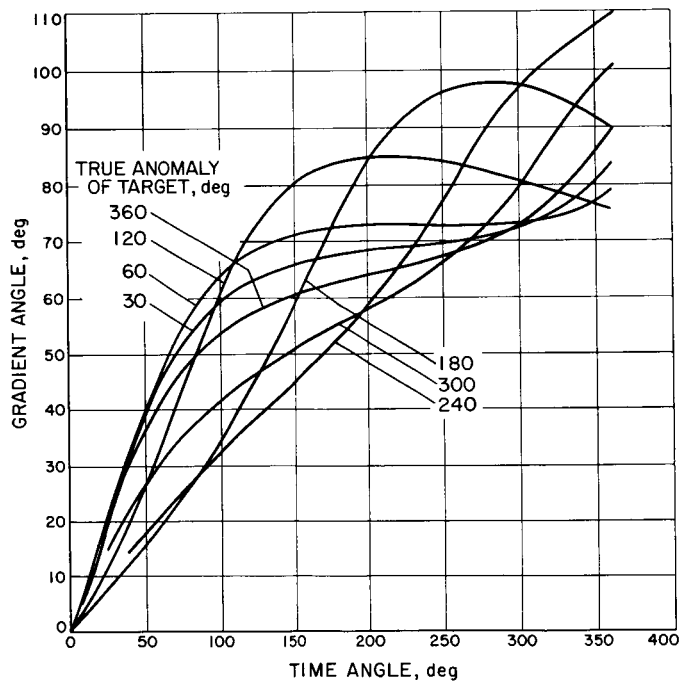


Fig. 15. Gradient angle vs time angle for eccentricity 0.25

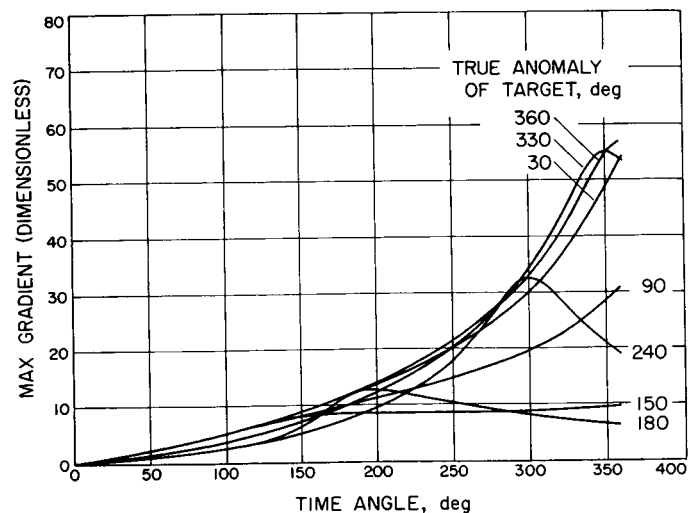


Fig. 17. Max gradient vs time angle for eccentricity 0.5

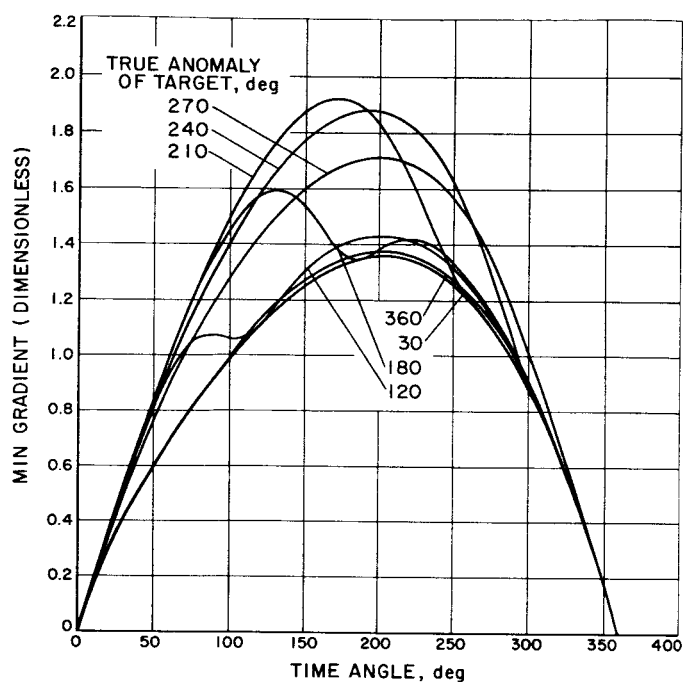


Fig. 18. Min gradient vs time angle for eccentricity 0.5

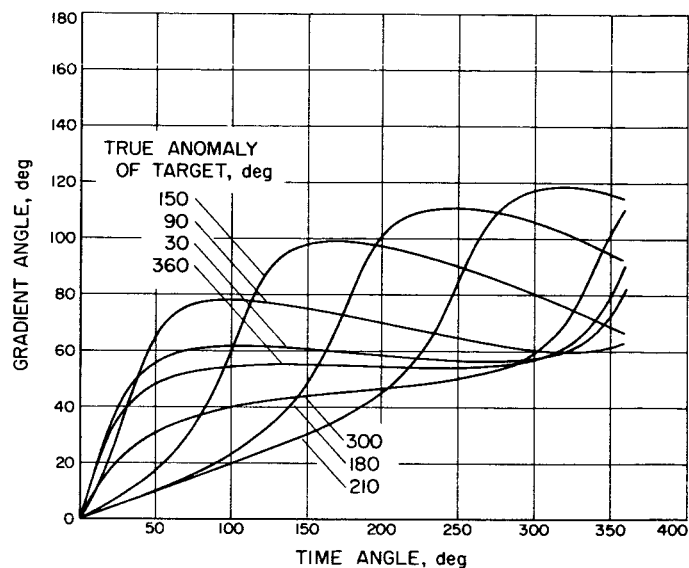


Fig. 20. Gradient angle vs time angle for eccentricity 0.5

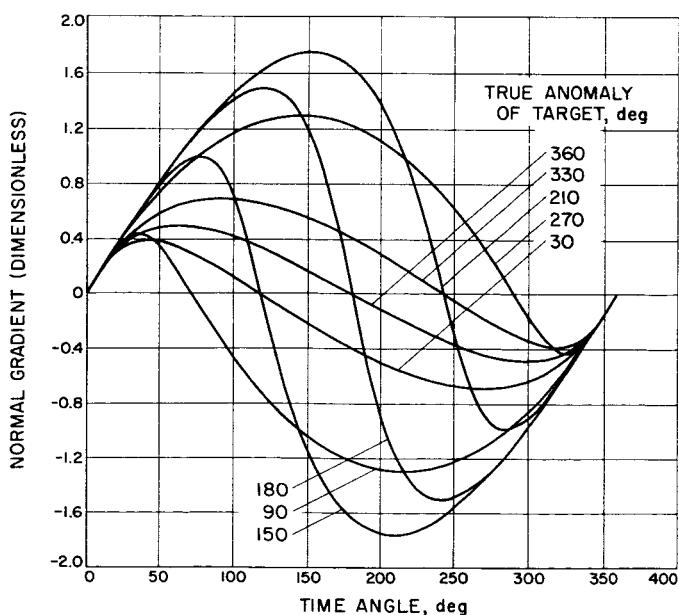


Fig. 19. Normal gradient vs time angle for eccentricity 0.5

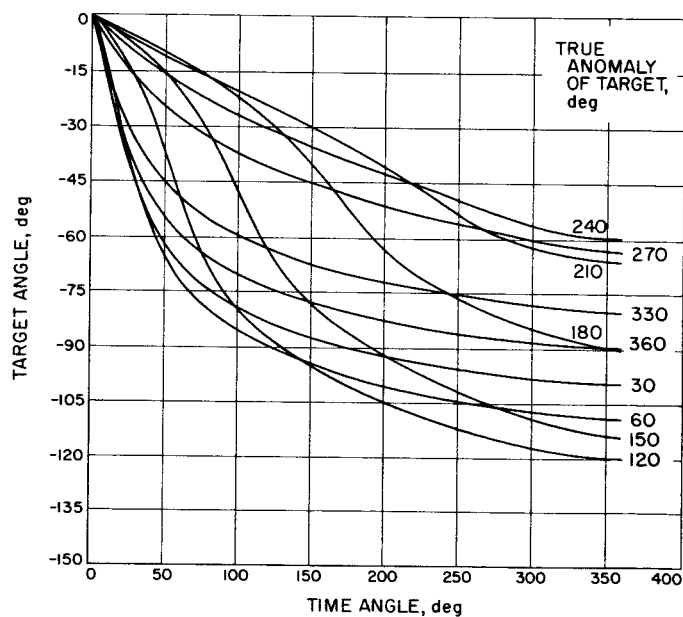


Fig. 21. Target angle vs time angle for eccentricity 0.5

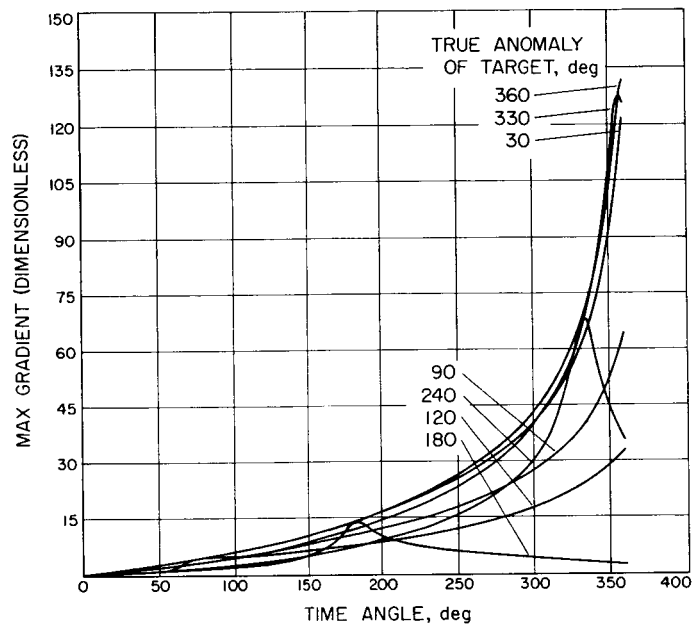


Fig. 22. Max gradient vs time angle for eccentricity 0.75

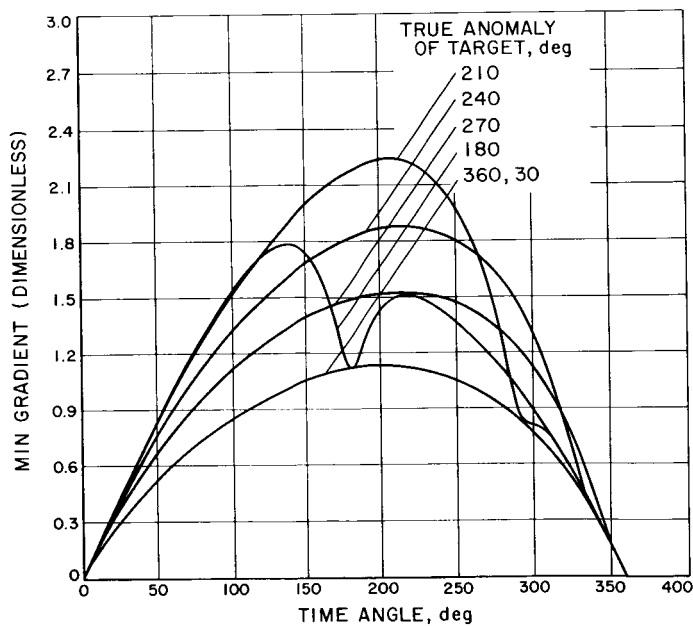


Fig. 23. Min gradient vs time angle for eccentricity 0.75

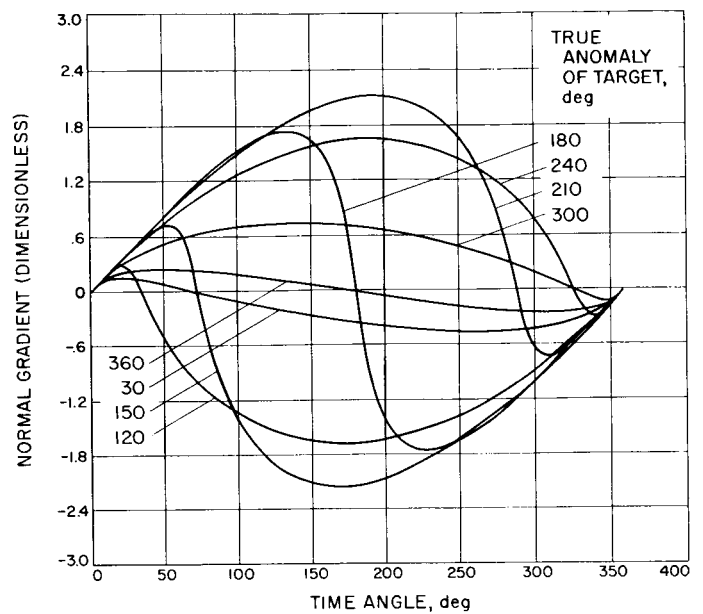


Fig. 24. Normal gradient vs time angle for eccentricity 0.75

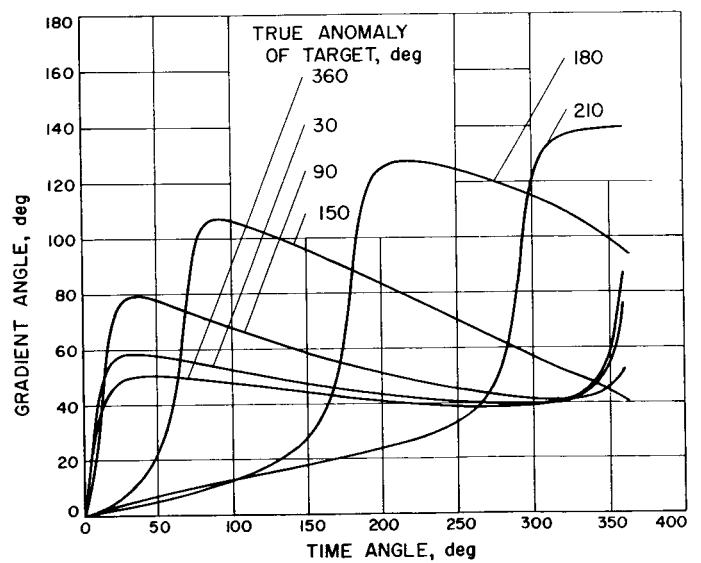


Fig. 25. Gradient angle vs time angle for eccentricity 0.75

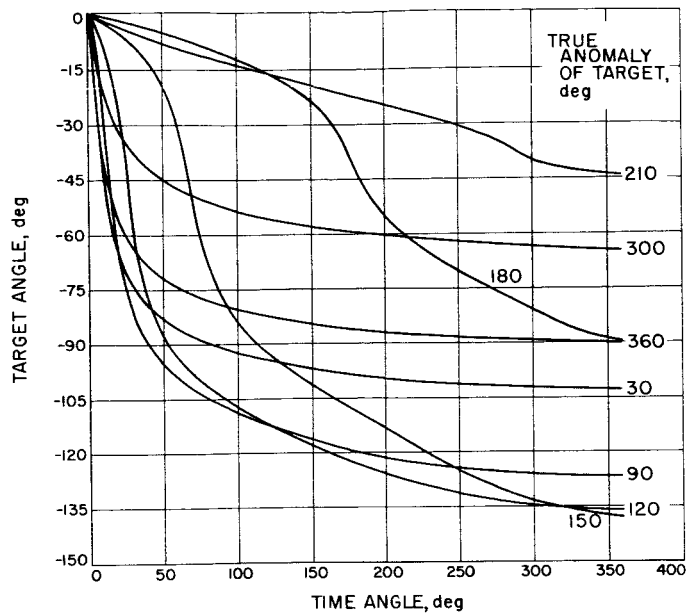


Fig. 26. Target angle vs time angle for eccentricity 0.75

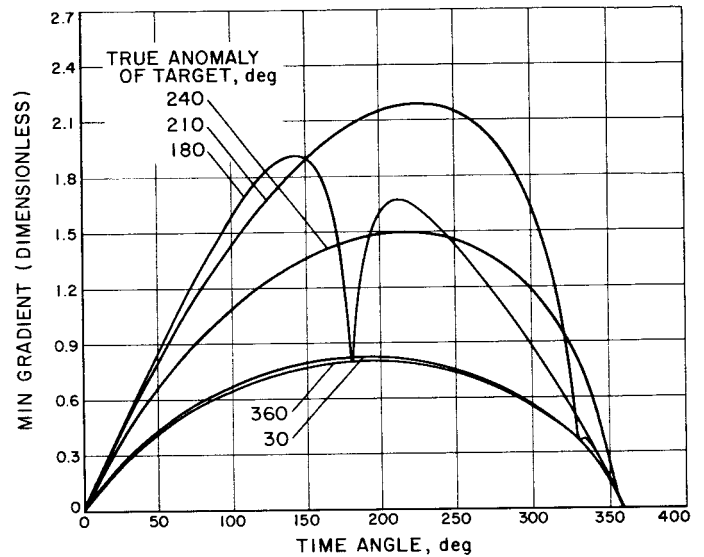


Fig. 28. Min gradient vs time angle for eccentricity 0.9

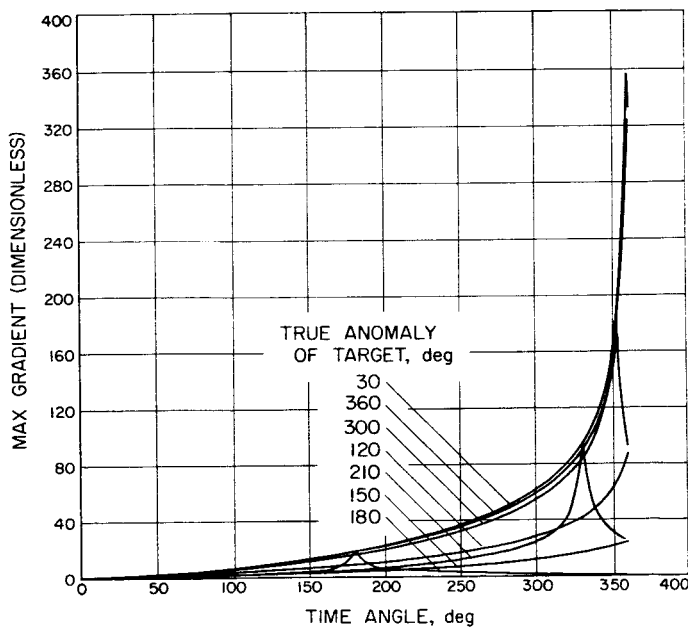


Fig. 27. Max gradient vs time angle for eccentricity 0.9

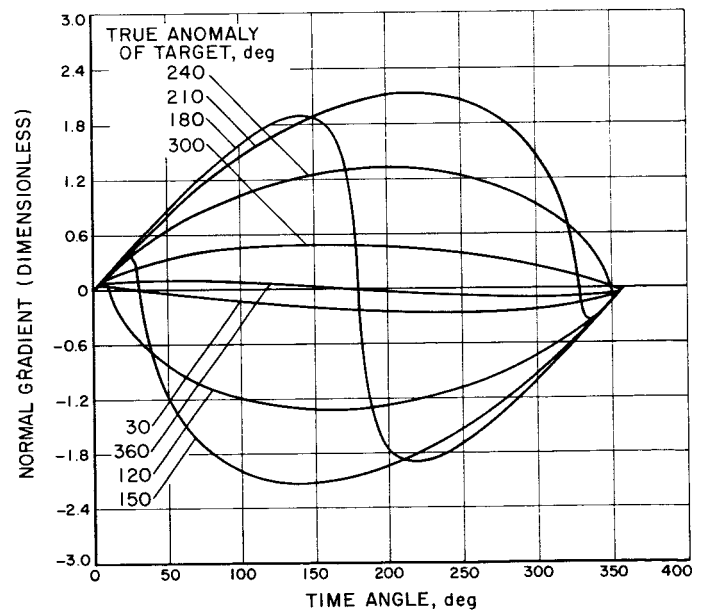


Fig. 29. Normal gradient vs time angle for eccentricity 0.9

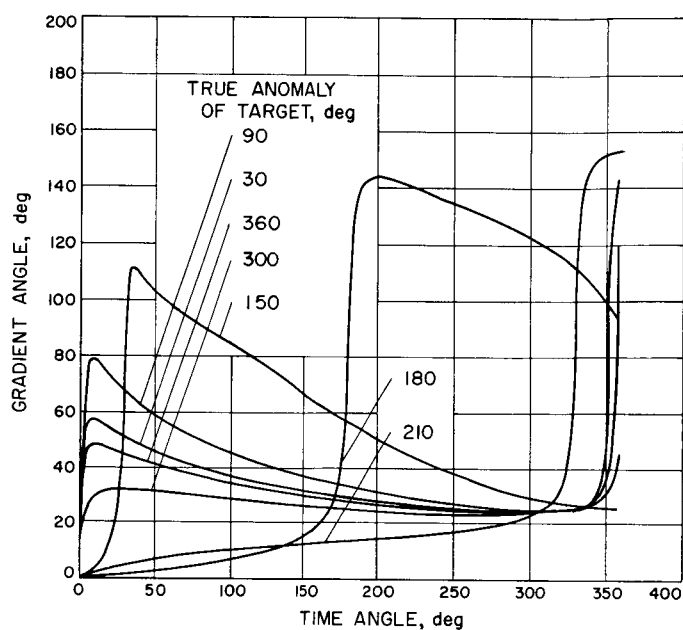


Fig. 30. Gradient angle vs time angle for eccentricity 0.9

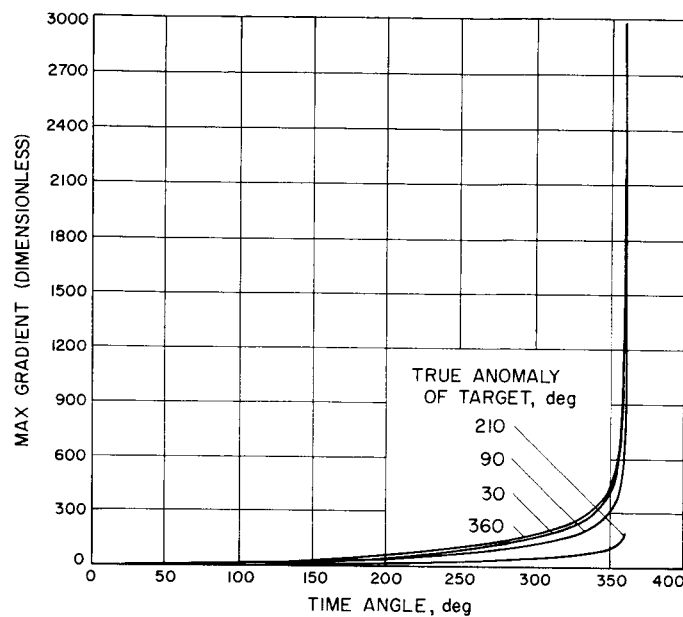


Fig. 32. Max gradient vs time angle for eccentricity 0.98741

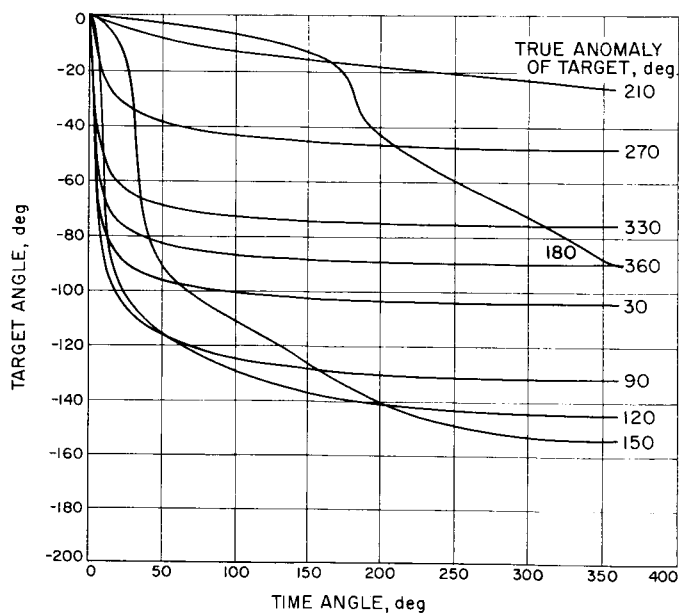


Fig. 31. Target angle vs time angle for eccentricity 0.9

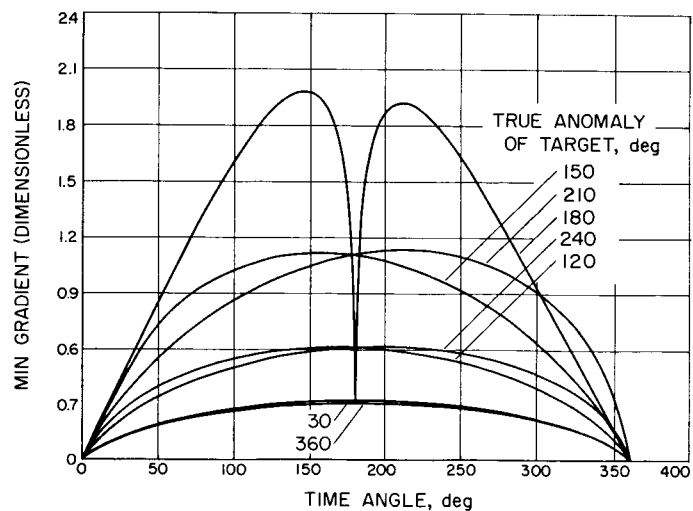


Fig. 33. Min gradient vs time angle for eccentricity 0.98741

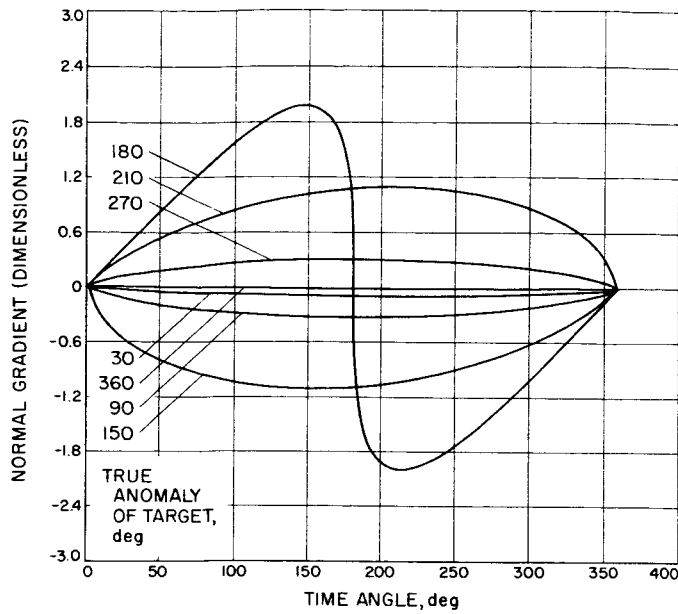


Fig. 34. Normal gradient vs time angle for eccentricity 0.98741

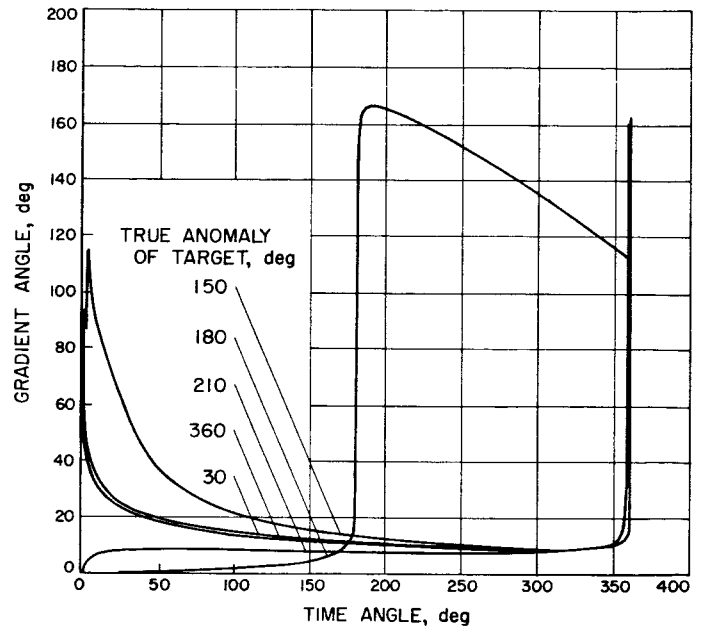


Fig. 35. Gradient angle vs time angle for eccentricity 0.98741

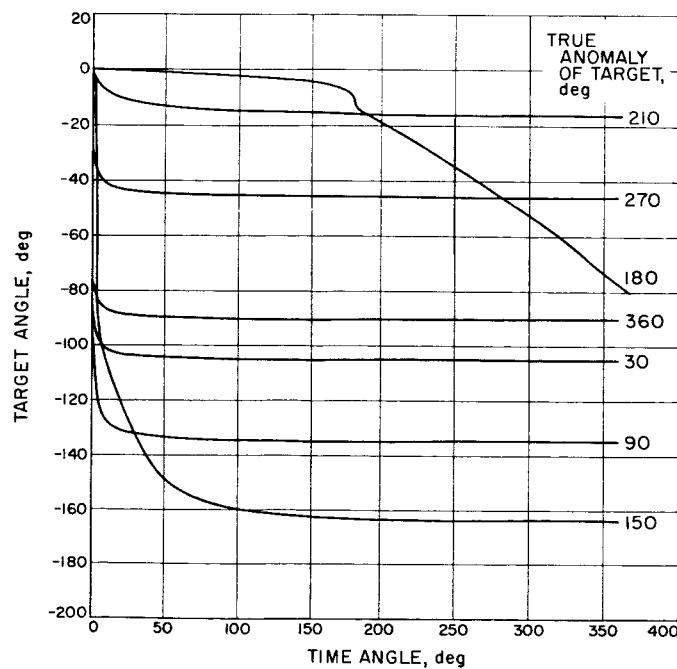


Fig. 36. Target angle vs time angle for eccentricity 0.98741

NOMENCLATURE

Column vectors are denoted by bold-face characters; small letters and the symbols E , F , and G are scalars; other capital letters are matrices; I is the identity matrix; the superscript T indicates the transpose of a vector or matrix; t is time; the symbol $\langle \dots \rangle$ indicates the statistical expectation of the quantity in braces; subscripts denote the time at which the indicated quantity is being considered.

Scalars

t	time
t_0	initial time (injection)
t_f	final time (at the target point)
r	magnitude of \mathbf{r}
v	magnitude of \mathbf{v}
μ	product of the gravitational constant and the mass of the central body
a	semimajor axis of the ellipse
e	eccentricity of the ellipse
ν	true anomaly
E	eccentric anomaly
ϕ_1, ϕ_2	angle coordinates (true anomalies, eccentric anomalies, or mean anomalies) of the space vehicle at times t_1 and t_2 , respectively
n	mean angular velocity
F, G, f, g	functions appearing in the derivation of the K matrix elements
λ_i	i th diagonal element of diagonalized K matrix
λ'_i	i th diagonal element of diagonalized K' matrix
λ^*_i	i th semiaxis of a dispersion ellipsoid
x, y, z	Cartesian coordinates, where the x and y components are in the standard plane of motion and x is in the direction of periapsis
k_{ij}	element of the K matrix
α_i	coordinate rotation angle that defines the N_i matrix
c, b, h	elements of the (KK^T) matrix
k	an index of constant probability

Vectors

\mathbf{r}	position of the spacecraft
\mathbf{v}	velocity of the spacecraft

NOMENCLATURE (Cont'd)

- \mathbf{q} coordinate vector of the spacecraft; thus $\mathbf{q}^T = (\mathbf{r}^T, \mathbf{v}^T)$
 \mathbf{g}_i a gradient vector; specifically, the i th row of the \hat{K} matrix
 \mathbf{e}_i basis vector for the x, y, z Cartesian coordinate system

Matrices

- Λ_x the covariance matrix of the subscripted quantity; thus $\Lambda_x = \langle \mathbf{x}\mathbf{x}^T \rangle$
 K_t the partial derivative matrix $\begin{bmatrix} \frac{\partial \mathbf{r}_t}{\partial \mathbf{v}_t} \end{bmatrix}$
 K'_t the factored K_t matrix; i.e., $K'_t = nK_t$
 \hat{K} the 2 by 2 K matrix resulting from considering only plane-of-motion coordinates
 U_i the partial derivative matrix $\begin{bmatrix} \frac{\partial \mathbf{r}_t}{\partial \mathbf{q}_t} \end{bmatrix}$
 N_i a rotation matrix constructed at time t_i

APPENDIX

Derivation of the Elements of K ,

Presented here is a derivation of relatively simple analytical expressions for the elements of the K matrix on an elliptic trajectory.

On an elliptic trajectory the vector \mathbf{r}_2 can be expressed in terms of $\mathbf{r}_1, \mathbf{v}_1$ and Δt in the form (Ref. 6)

$$\mathbf{r}_2 = f(\Delta t, \mathbf{r}_1, \mathbf{v}_1) \mathbf{r}_1 + g(\Delta t, \mathbf{r}_1, \mathbf{v}_1) \mathbf{v}_1 \quad (\text{A-1})$$

where

$$f = \frac{a}{r_1} (\cos \Delta E - 1) + 1 \quad (\text{A-2})$$

$$g = \Delta t - \frac{\Delta E - \sin \Delta E}{n}$$

If \mathbf{v}_1 is perturbed by an amount $\delta \mathbf{v}_1$, the first-order perturbation of $\mathbf{r}_2, \delta \mathbf{r}_2$, holding Δt fixed, is given by

$$\delta \mathbf{r}_2 = \delta f \mathbf{r}_1 + \delta g \mathbf{v}_1 + g \delta \mathbf{v}_1 \quad (\text{A-3})$$

Using the results of Ref. 6 with some change of variables we obtain

$$\delta f = f_1 \mathbf{r}_1 \cdot \delta \mathbf{v}_1 + f_2 \mathbf{v}_1 \cdot \delta \mathbf{v}_1 \quad (\text{A-4})$$

$$\delta g = g_1 \mathbf{r}_1 \cdot \delta \mathbf{v}_1 + g_2 \mathbf{v}_1 \cdot \delta \mathbf{v}_1$$

with

$$\begin{aligned}
 f_1 &= -\frac{\sin \Delta E (\cos \Delta E - 1)}{r_1 r_2 n} \\
 f_2 &= \frac{1}{ar_1 n^2} \left\{ 2 (\cos \Delta E - 1) + \frac{a}{r_2} \sin \Delta E \left[2ng + 3\Delta E \right. \right. \\
 &\quad \left. \left. - \left(\frac{r_1}{a} + 3 \right) \sin \Delta E \right] \right\} \\
 g_1 &= \frac{(\cos \Delta E - 1)^2}{r_2 a n^2} \\
 g_2 &= \frac{-1}{a^2 n^3} \left\{ \frac{a}{r_2} (\cos \Delta E - 1) \left[2ng + 3\Delta E \right. \right. \\
 &\quad \left. \left. - \left(\frac{r_1}{a} + 3 \right) \sin \Delta E \right] + 3 (\Delta E - \sin \Delta E) \right\} \quad (A-5)
 \end{aligned}$$

Since the coordinates in the standard plane of the trajectory are not coupled to out-of-plane coordinates, it is convenient to assign a coordinate system for the position and velocity vectors such that one of the coordinate axes is perpendicular to the plane of motion. We therefore let

$$\begin{aligned}
 \mathbf{r}_1 &= x_1 \mathbf{e}_1 + y_1 \mathbf{e}_2 \\
 \mathbf{r}_2 &= x_2 \mathbf{e}_1 + y_2 \mathbf{e}_2 \\
 \mathbf{v}_1 &= \dot{x}_1 \mathbf{e}_1 + \dot{y}_1 \mathbf{e}_2 \\
 \delta \mathbf{v}_1 &= \delta \dot{x}_1 \mathbf{e}_1 + \delta \dot{y}_1 \mathbf{e}_2 + \delta \dot{z}_1 \mathbf{e}_3
 \end{aligned} \quad (A-6)$$

where \mathbf{e}_1 and \mathbf{e}_2 are in-plane orthogonal unit vectors, and \mathbf{e}_3 is in the out-of-plane direction. For the K matrix defined by

$$\begin{bmatrix} \delta x_2 \\ \delta y_2 \\ \delta z_2 \end{bmatrix} = K \begin{bmatrix} \delta \dot{x}_1 \\ \delta \dot{y}_1 \\ \delta \dot{z}_1 \end{bmatrix} = \begin{bmatrix} k_{11} & k_{12} & k_{13} \\ k_{21} & k_{22} & k_{23} \\ k_{31} & k_{32} & k_{33} \end{bmatrix} \begin{bmatrix} \delta \dot{x}_1 \\ \delta \dot{y}_1 \\ \delta \dot{z}_1 \end{bmatrix} \quad (A-7)$$

we immediately obtain

$$\begin{aligned}
 k_{11} &= F_1 x_1 + G_1 \dot{x}_1 + g \\
 k_{12} &= F_2 x_1 + G_2 \dot{x}_1 \\
 k_{13} &= 0 \\
 k_{21} &= F_1 y_1 + G_1 \dot{y}_1 \\
 k_{22} &= F_2 y_1 + G_2 \dot{y}_1 + g \\
 k_{23} &= 0 \\
 k_{31} &= 0 \\
 k_{32} &= 0 \\
 k_{33} &= g
 \end{aligned} \quad (A-8)$$

where

$$\begin{aligned}
 F_1 &= f_1 x_1 + f_2 \dot{x}_1 \\
 F_2 &= f_1 y_1 + f_2 \dot{y}_1 \\
 G_1 &= g_1 x_1 + g_2 \dot{x}_1 \\
 G_2 &= g_1 y_1 + g_2 \dot{y}_1
 \end{aligned} \quad (A-9)$$

Although the expressions developed in this Appendix hold only when the same nonrotating Cartesian coordinate system is used for both $\delta \mathbf{v}_1$ and $\delta \mathbf{r}_2$, the modification of the K matrix for any other desired coordinate systems is easily carried out by the multiplication of appropriate transformation matrices.

It is noteworthy that the eccentricity e does not appear explicitly in Eq. (A-8). These equations, therefore, are accurate for the entire range of e -values for elliptic orbits.

REFERENCES

1. Richard, R. E., et al., *Earth-Moon Trajectories*, Technical Report No. 32-503, Jet Propulsion Laboratory, Pasadena, California, August 1963.
2. Clarke, V. C., Jr., et al., *Design Parameters for Ballistic Interplanetary Trajectories*, Technical Report No. 32-77, Jet Propulsion Laboratory, Pasadena, California, January 1963.
3. Piaggi, E. G., "Some Properties of Lunar Differential Corrections and Their Implications to Guidance Analysis," *Space Programs Summary No. 37-21*, Vol. 4, p. 11, Jet Propulsion Laboratory, Pasadena, California, June 1963.
4. Noton, A. R. M., *The Statistical Analysis of Space Guidance Systems*, Technical Memorandum No. 33-15, Jet Propulsion Laboratory, Pasadena, California, June 1960.
5. Noton, A. R. M., E. Cutting, and F. L. Barnes, *Analysis of Radio-Command Mid-Course Guidance*, Technical Report No. 32-28, Jet Propulsion Laboratory, Pasadena, California, September 1960.
6. Pines, S., "Variation of Parameters for Elliptic and Near Circular Orbits," *The Astronomical Journal*, Vol. 66, No. 1, p. 5.